Colloid Polym Sci 279:449–458 (2001)

ORIGINAL CONTRIBUTION

S. Papp
I. Dékány

Structural properties of palladium nanoparticles embedded in inverse microemulsions

Received: 17 July 2000
Accepted: 5 October 2000

S. Papp · I. Dékány (✉)
Department of Colloid Chemistry
and Nanostructured Materials
Research Group of the
Hungarian Academy of Science
University of Szeged
Aradi Vértanúk tere 1
H 6720 Szeged, Hungary
e-mail: i.dekany@chem.u-szeged.hu

Abstract Pd nanoparticles were synthesized by reduction of palladium acetate by ethanol in systems containing tetrahydrofuran (THF) as dispersion medium and tetradodecylammonium bromide (TDABr) surfactant as stabilizer. The polar phase (ethanol) acts at the same time as reducing agent. THF/TDABr/H_2O inverse microemulsions containing micelles of various sizes were also prepared, and the structure of complex liquids was studied by density measurements. Sols containing nanosize Pd^0 particles were synthesized within the water droplets of this micellar system. The stabilized Pd^0/surfactant system was characterized by density measurements, absorption spectroscopy, and transmission electron microscopy. The stabilizing surfactant layer adsorbed on the liquid/liquid interface and on the surface of the nanoparticles (i.e., the liquid/solid interface) significantly reduced the excess volume for the palladium nanodispersion in organic solvent.

Key words Pd nanoparticles · Microemulsions · Stabilization of colloid particles · Excess volume of solution · Surfactants · TEM

Introduction

Preparation and investigation of nanosize particles is gaining increasing significance in both scientific and technological respects, since their physical and chemical properties are markedly different from those of larger particles of identical composition.

Several physical and chemical methods are commonly known for the preparation of nanoparticles, e.g., controlled crystal or cluster growth on supports or in microemulsions, molecular epitaxy, controlled colloid synthesis, and various high-intensity grinding techniques. Since the particle size may be conveniently controlled by varying the conditions of preparation, catalysts of pre-planned activity or semiconductors of desired size with the required forbidden band energy can also be prepared [1–3]. The aim of the present work was to prepare Pd nanoparticles within the polar droplets of inverse microemulsions. The systems obtained were characterized by density measurements, UV-VIS absorption spectroscopy, and transmission electron microscopy.

Within the droplets (hydrophylic pool) of inverse microemulsion(s), the so-called nanophase reactor, nanophase materials of various qualities with controlled particle size can be prepared [4–10]. The inner radius of the droplet is determined by the composition and structure of the microemulsion. Thus, inverse microemulsions with the desired micelle size must be prepared by selecting the appropriate molar ratio (W_0) of polar phase and surfactant [4, 8–10]. The radius R of the water droplet is calculated by the following equations [11–16]:

$$V_{drop} = 4/3\pi R^3 = V_{H_2O} + V_h \quad (1)$$

i.e., the volume of the droplet is the sum of the volume of water, V_{H_2O}, and the hydrophilic head-groups of the surfactant molecules, V_h. With $a_m = 4\pi R^2$, the average surface of a droplet, we obtain

$$R^3/3R^2 = V_{H_2O}/a_m + V_h/a_m \quad (2)$$

Let V_w be the space requirement of one water molecule (29.9 $Å^3$) and a_h the surface requirement of one polar head group on the interface. Thus $V_h/a_m = V_h/a_h$ and $V_{H_2O}/a_m = V_{H_2O}W_0/a_h$, and it follows

$$R = 3(V_{H_2O}W_0 + V_h)/a_h \quad (3)$$

In other words, the inner radius of the droplet is determined by the composition and structure of the microemulsion.

According to the literature, an increasing $[H_2O]/[AOT]$ molar ratio, while keeping other parameters constant, increases the particle size [17]. Various metal ion reduction procedures were described for the preparation of transition metal particles. In most of these methods, aggregation of the emerging particles is prevented by steric stabilization, i.e., the surface of the nanoparticles is coated by an adsorption layer. This thick, compact adsorption layer sterically protects the particles from coagulation by collisions. Salts and oxides of transition metals were reduced in organic medium (toluene, tetrahydrofuran) using tetrahydroborates of alkali metals or hydrotriorganoborates of alkali earth metals [18–22]. The particles formed were stabilized by tetraalkylammonium halogenides [18].

The length of the alkyl chains attached to metal nanoparticles is usually C_6–C_{20}. Since the local concentration of the tetraalkylammonium ions formed in the vicinity of the site of reduction is extremely large, they are rapidly adsorbed on the surface of the freshly reduced, negatively charged metal particles, which prevents further aggregation. This method has also been used for the preparation of the colloidal alloys of various metals by simultaneous reduction of the components. In addition to stabilizing agents of the NR_4 type, other association colloids are also used in the course of the preparation of metals of subcolloidal size and their alloys. Esumi et al. [23] synthesized Pd-Pt bimetallic colloids in cyclohexane or toluene medium in the presence of trioctylphosphine oxide (TOPO) or distearyl-dimethylammonium chloride (DDAC). Hydrazine and sodium borohydride were used as reducing agents. Reduction by hydrazine yielded 20–30-nm particles whereas with borohydride particles of 5–8 nm diameter were obtained.

Au and Pt colloids were prepared in biphasic systems by Fink et al. [24]: precursor salts dissolved in water were dispersed in surfactant containing organic medium, and reduced. Examples are $HAuCl_4$ in toluene/water containing tetraalkylammonium bromide (C_6; C_{18}) and reduction by Na-borohydride, H_2PtCl_6 in chloroform/water or cyclohexane/water via reduction by formaldehyde or benzaldehyde [24, 25]. Boutonnet et al. [26] reported the preparation of monodisperse metal particles (Pt, Pd, Rh, Ir) by reduction of metal salts dissolved in the aqueous microphase, using octanol, hexane, isooctane, *n*-heptane, or hexadecane as dispersion medium and cationic surfactants as stabilizers.

Materials and methods

Materials

The following materials were used for the experiments: tetrahydrofuran (THF, C_4H_8O, 99.8%, Carlo Erba, $M_r = 72.108$, $\rho = 0.889$ g/ml), ethanol (EtOH, C_2H_6O, 99.8%, Reanal, $M_r = 46.07$, $\rho = 0.79$ g/ml), palladium acetate ($Pd(OAc)_2$, 99%,

Table 1 Composition of inverse microemulsions

Symbol	Compound
$r(H_2O)$ = 5 nm; W_0 = 11.1	
SW1/1	THF/TDABr(4.54 mmol/l)/H_2O(50.2 mmol/l)
SW2/1	THF/TDABr(9.1 mmol/l)/H_2O(100.8 mmol/l)
SW3/1	THF/TDABr(13.6 mmol/l)/H_2O(151.2 mmol/l)
$r(H_2O)$ = 10 nm; W_0 = 34.5	
SW1/2	THF/TDABr(4.54 mmol/l)/H_2O(156.6 mmol/l)
SW2/2	THF/TDABr(9.1 mmol/l)/H_2O(313.2 mmol/l)
SW3/2	THF/TDABr(13.6 mmol/l)/H_2O(469.8 mmol/l)
$r(H_2O)$ = 20 nm; W_0 = 81.3	
SW1/3	THF/TDABr(4.54 mmol/l)/H_2O(369.1 mmol/l)
SW2/3	THF/TDABr(9.1 mmol/l)/H_2O(738.2 mmol/l)
SW3/3	THF/TDABr(13.6 mmol/l)/H_2O(1107.3 mmol/l)
r(EtOH) = 5.6 nm; W_0 = 4.3	
SE1/1	THF/TDABr(4.54 mmol/l)/EtOH(19.5 mmol/l)
SE2/1	THF/TDABr(9.1 mmol/l)/EtOH(39.1 mmol/l)
SE3/1	THF/TDABr(13.6 mmol/l)/EtOH(58.5 mmol/l)
r(EtOH) = 12 nm; W_0 = 13.5	
SE1/2	THF/TDABr(4.54 mmol/l)/EtOH(61.3 mmol/l)
SE2/2	THF/TDABr(9.1 mmol/l)/EtOH(122.8 mmol/l)
SE3/2	THF/TDABr(13.6 mmol/l)/EtOH(183.6 mmol/l)
r(EtOH) = 24.8 nm; W_0 = 31.8	
SE1/3	THF/TDABr(4.54 mmol/l)/EtOH(144.4 mmol/l)
SE2/3	THF/TDABr(9.1 mmol/l)/EtOH(289.4 mmol/l)
SE3/3	THF/TDABr(13.6 mmol/l)/EtOH(432.5 mmol/l)

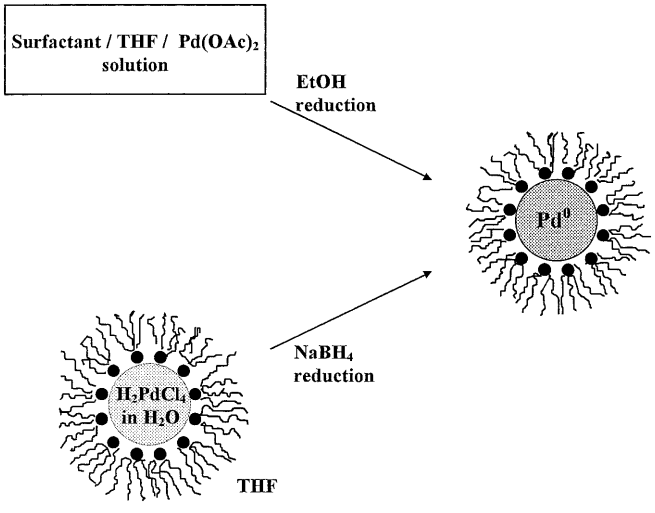

Fig. 1 Preparation of nanoparticles in surfactant solution and microemulsion

Merck, $M_r = 224.49$), tetradodecylammonium bromide (TDABr, $C_{48}H_{100}BrN$, 99%, Fluka, $M_r = 224.29$).

Preparation of inverse microemulsions

The mass ratio of water and surfactant necessary for the preparation of w/o type microemulsions with a water droplet radius of 2.5–25 nm was calculated by Eq. (3). It was assumed that the four alkyl chains of TDABr point towards the organic phase. The necessary data are: chain length of TDA^+ cations $l = 2.16$ nm, surfactant volume $V = 1.548$ nm^3, average volume of the polar head-group $V_h = 0.3678$ nm^3, its surface requirement, $a_h = 0.42$ nm^2. The calculated density of the surfactant was 0.83 g/cm^3. According to Eq. (3), microemulsions with water droplet radii of 5 nm, 10 nm, and 20 nm were prepared at water-surfactant ratios of $W_0 = 11.1$; 34.5; 81.3. Microemulsions of THF-surfactant-ethanol were also made up at ethanol-surfactant ratios of $W_0 = 4.3$; 13.5; 31.8 (Table 1).

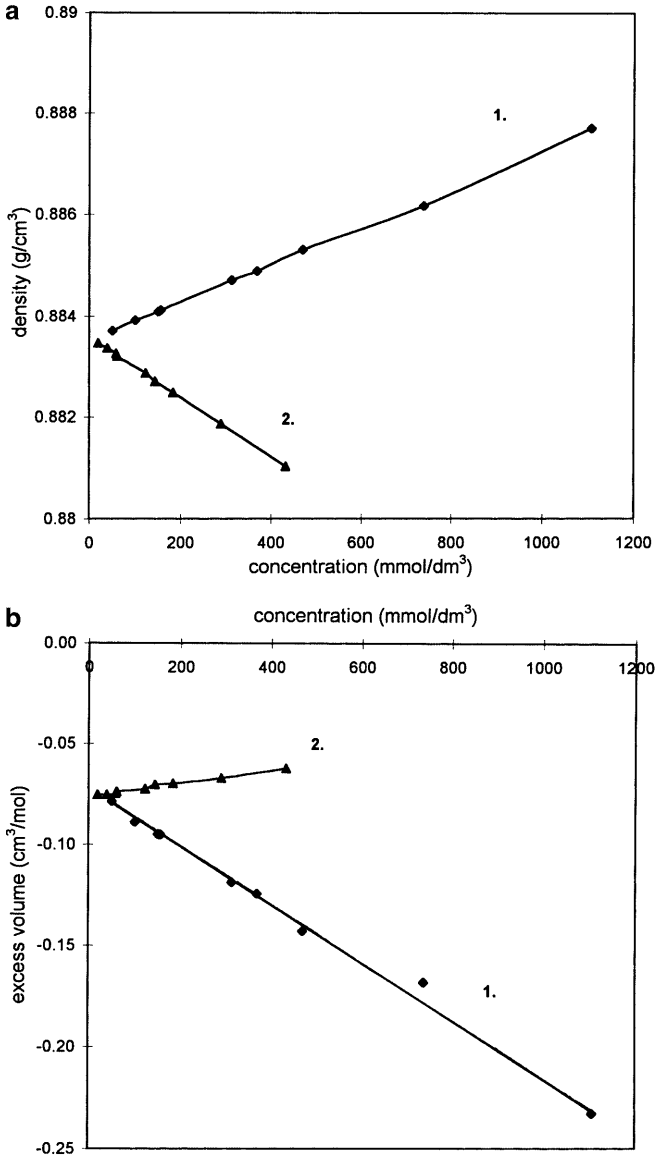

Fig. 2 **a** Density for binary systems THF/water and THF/EtOH solutions by different concentration. **b** Excess volume calculated from density functions (Eq. 4): (1) water, (2) ethanol as the polar component solution

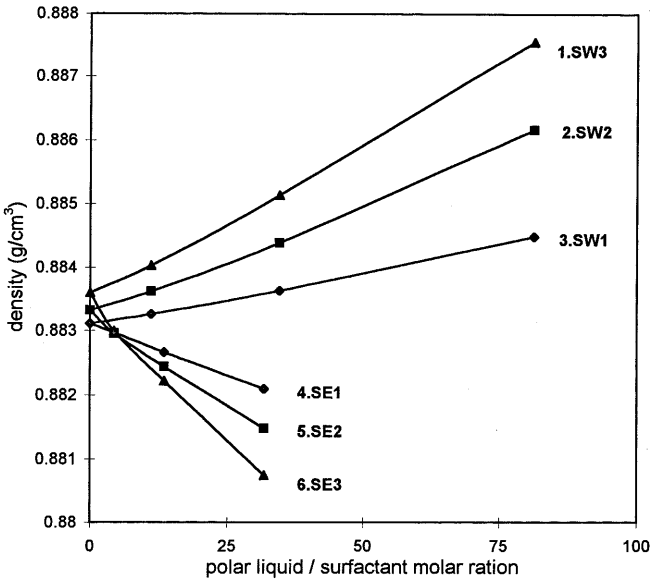

Fig. 3 The density of ternary systems THF/TDABr/H_2O and THF/TDABr/EtOH: 1, SW3; 2, SW2; 3, SW1; 4, SE1; 5, SE2; 6, SE3 as a function of water and ethanol/surfactant molar ration

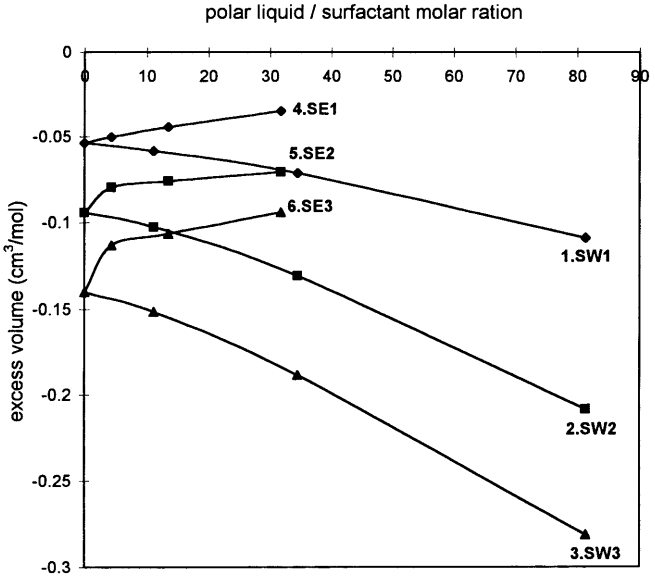

Fig. 4 The excess volume for ternary systems THF/TDABr/H_2O and THF/TDABr/EtOH: 1, SW3; 2, SW2; 3, SW1; 4, SE1; 5, SE2; 6, SE3 calculated from Eq. (5) as a function of water and ethanol/surfactant molar ration

Preparation of Pd^0 nanoparticles in THF/water/TDABr systems

Pd^0 nanosol was prepared at 25 °C (SE3/2) ensuring a particle size of r = 10 nm in the following way. In 11-cm^3 aliquots of THF-surfactant solution, 0.10 mmol, 0.15 mmol, or 0.20 mmol of $Pd(OAc)_2$ were dissolved, followed by the addition of calculated amounts of ethanol. After the addition of ethanol, the systems were agitated by magnetic stirring for 60 min. During this time reduction started in the sample containing 0.2 mmol of Pd acetate and a dark-colored sol was formed. After one day the reaction was also completed in the other two samples (0.15 mmol and 0.1 mmol of Pd-acetate). (It should be noted that the reaction never started in the system containing 0.05 mmol of Pd-acetate.) The synthesis route is shown in Fig. 1.

Pd^0 nanosols were also prepared in aqueous THF/surfactant microemulsions ($W_0 = 448$, r = 200 nm) at 25 °C. A volume of 1 cm^3 of acidic 10 mmol/l, 15 mmol/l, or 20 mmol/l $PdCl_2$ was added to 10 cm^3 of 13.6 mmol/l surfactant solution and, with constant stirring, the system was reduced by 0.1 cm^3 of 0.4 mol/l $NaBH_4$ solution. Particle formation started after 5–8 min.

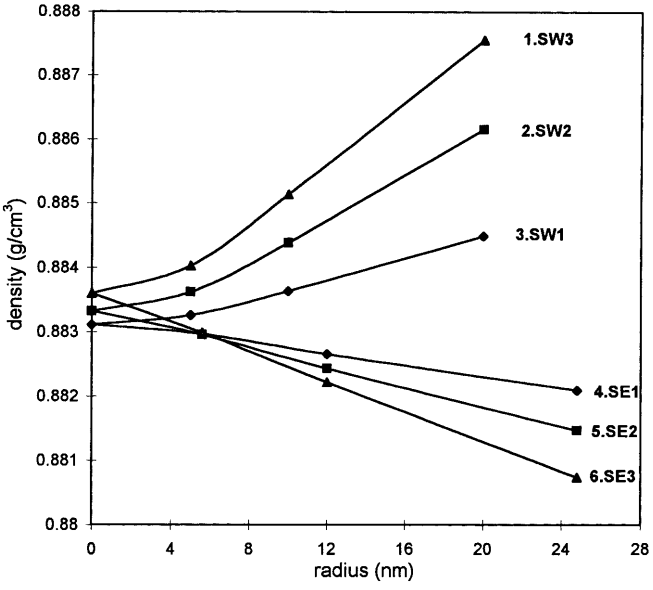

Fig. 5 The density of ternary systems THF/TDABr/H_2O and THF/TDABr/EtOH: 1, SW3; 2, SW2; 3, SW1; 4, SE1; 5, SE2; 6, SE3 for different droplet radii

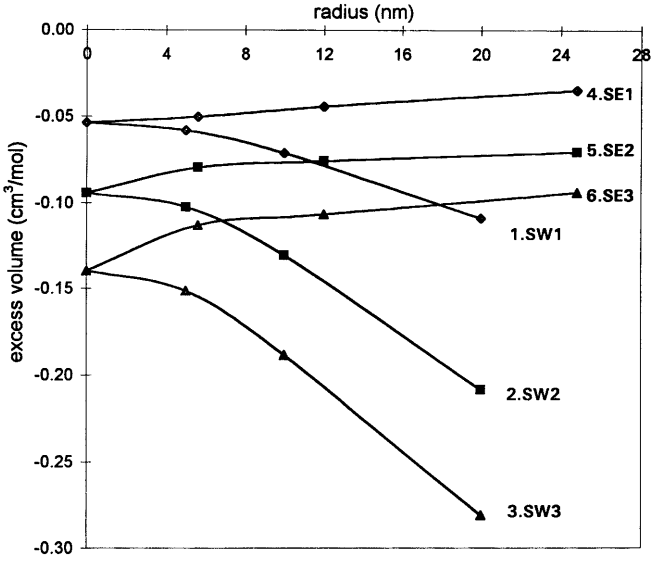

Fig. 6 The excess volume for ternary systems THF/TDABr/H_2O and THF/TDABr/EtOH; 1, SW3; 2, SW2; 3, SW1; 4, SE1; 5, SE2; 6, SE3 calculated from Eq. (5)

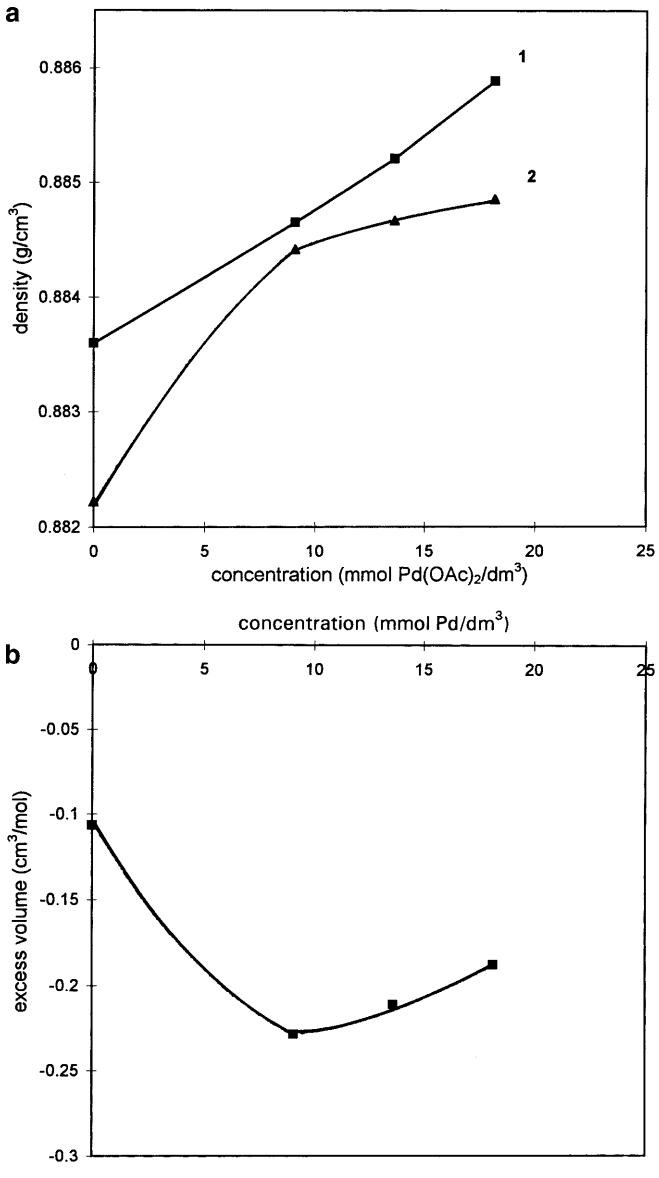

Fig. 7 **a** Influence of $Pd(OAc)_2$ on the density of solution (1), or nanosols (2): 1, before reduction for systems Pd^{2+}/THF/TDABr; 2, after reduction for systems Pd^0/THF/TDABr/EtOH. **b** Influence of Pd^0 concentration on the excess volume, Pd/THF/TDABr/EtOH (Pd^0S1,2,3), calculated from curve 2 on Fig. 7a by Eq. (6)

Methods

Density measurements and excess volumes

The molar excess volumes (V_m^E) of the systems are calculated from density and composition by of the following equation:

$$V_m^E = [(x_1 \times M_1 + x_2 \times M_2)/\rho_{1,2}] - [x_1 \times M_1/\rho_1] - [x_2 \times M_2/\rho_2] \quad (4)$$

where M(i = 1, 2) is the molar mass of the pure components, x their molar fraction, ρ their density, and $\rho_{1,2}$ is the actual density of the system. The above equation is formulated for two-component systems. In the case of three or four components, one or two additional terms were added:

$$V_m^E = [(x_1 \times M_1 + x_2 \times M_2 + x_3 \times M_3)/\rho_{1,2,3}] - [x_1 \times M_1/\rho_1] - [x_2 \times M_2/\rho_2] - [x_3 \times M_3/\rho_3] \quad (5)$$

$$V_m^E = [(x_1 \times M_1 + x_2 \times M_2 + x_3 \times M_3 + x_4 \times M_4)/\rho_{1,2,3,4}] - [x_1 \times M_1/\rho_1] - [x_2 \times M_2/\rho_2] - [x_3 \times M_3/\rho_3] - [x_4 \times M_4/\rho_4] \quad (6)$$

Densities of liquids and microemulsions were measured in a computer-controlled Anton Paar DMA 58 density meter at 25 ± 0.01°C. Density measurement is based on highly accurate frequency measurement. The density of the complex liquid studied is calculated by the apparatus from the change in frequency.

UV-VIS absorption spectroscopy

UV-VIS spectroscopy was carried out in a dual-beam Uvikon 930 spectrophotometer at 25 ± 0.5 °C.

Pd^0 sols were studied in 10-mm quartz cuvettes. The system to be studied was placed in one light path, the reference system in the other, and the difference spectrum was recorded over the range 300–600 nm.

Transmission electron microscopy

Transmission electron microscopy (TEM) pictures were taken using a CM-10 Philips electron microscope, using a voltage of 100 kV. Samples were suspended in ethanol and spread on copper grids coated with Fromwar foil.

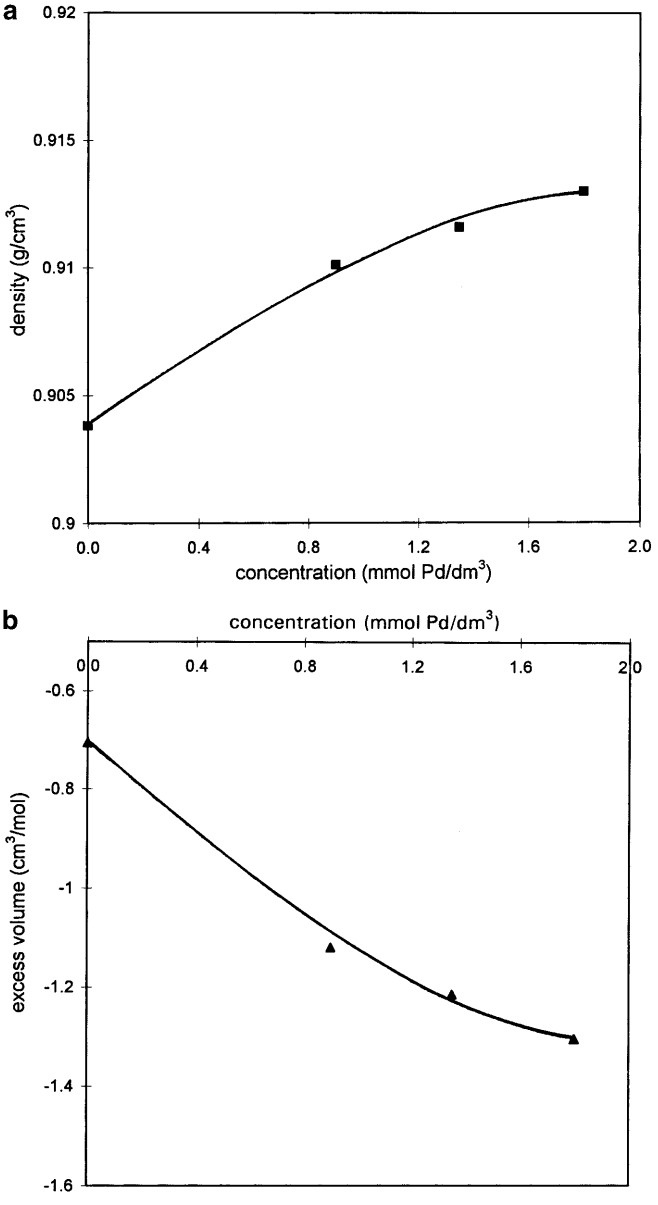

Fig. 8 **a** Influence of $PdCl_2$ concentration on the density, Pd^0/THF/TDABr/H_2O (Pd^0S4,5,6). **b** Influence of $PdCl_2$ concentration on the excess volume, Pd^0/THF/TDABr/H_2O (Pd^0S4,5,6) calculated from the density curve in Fig. 8a by Eq. (6)

Results and discussion

Densitometry

The density of systems free of surfactant as a function of the concentration of the water or ethanol added is presented in Fig. 2a. As is expected, the density is increased by the addition of water and decreased by that of ethanol. There is a marked difference, however, in the values of the excess volumes V_m^E (Fig. 2b). The incor-

Table 2 Composition of inverse microemulsion with Pd^{2+} precursors and with embedded Pd^0 nanoparticles after reduction

Symbol	Compound
r(EtOH) = 10 nm; before reduction	
Pd^{+2}S1	Pd^{+2}(9.1 mmol/l)/THF/TDABr
Pd^{+2}S2	Pd^{+2}(13.6 mmol/l)/THF/TDABr
Pd^{+2}S3	Pd^{+2}(18.2 mmol/l)/THF/TDABr
r(EtOH) = 10 nm; after reduction	
Pd^0S1	Pd^0(9.1 mmol/l)/THF/TDABr
Pd^0S2	Pd^0(13.6 mmol/l)/THF/TDABr
Pd^0S3	Pd^0(18.2 mmol/l)/THF/TDABr
r(H_2O) = 200 nm; after reduction	
Pd^0S4	Pd^0(0.9 mmol/l)/THF/TDABr
Pd^0S5	Pd^0(1.36 mmol/l)/THF/TDABr
Pd^0S6	Pd^0(1.8 mmol/l)/THF/TDABr

poration of water in the THF-containing system significantly reduces the excess volume, while in the system containing ethanol the excess volume, although negative, does not change considerably with increasing ethanol concentration.

The actual density values measured in THF/water microemulsions stabilized with tetradodecylammonium bromide increases with both the surfactant (S) and water (W) content, while in the ethanol-containing systems the density decreases not only with increasing ethanol but also with increasing surfactant concentrations (Fig. 3). According to Fig. 4, the excess volumes are negative in the presence of ethanol, which means that, in all cases, the addition of surfactant induces a structural changes

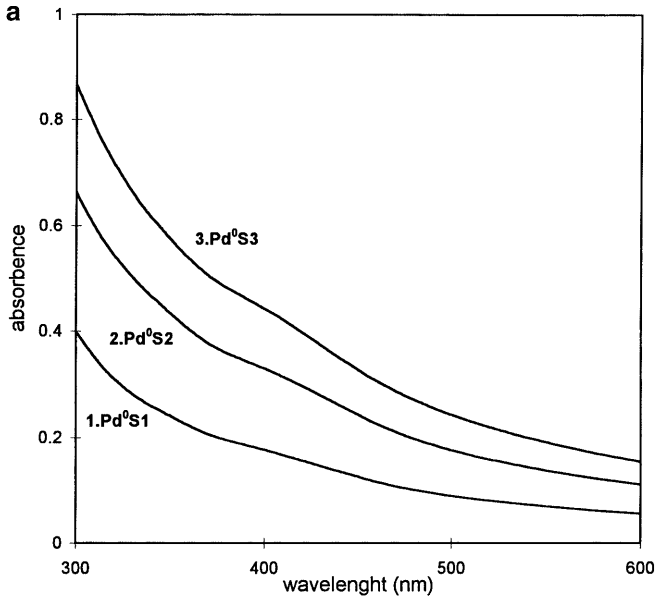

Fig. 9 **a** UV-VIS spectra of TDABr stabilized Pd^0 nanoparticles in THF at different Pd^0 concentration: 1, Pd^0S1; 2, Pd^0S2; 3, Pd^0S3. **b** Double logarithmic plots of the spectra of TDABr stabilized Pd^0 nanoparticles in THF (normalized at $\lambda = 450$ nm with $A = 1$) at different Pd^0 concentrations: 1, Pd^0S1; 2, Pd^0S2; 3, Pd^0S3

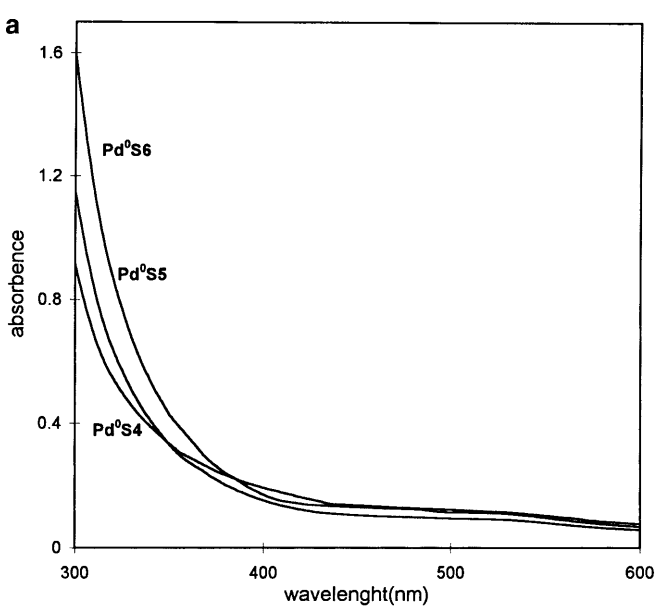

Fig. 10 **a** UV-VIS spectra of TDABr stabilized Pd^0 nanoparticles in THF at different Pd^0 concentrations: 1, Pd^0S4; 2, Pd^0S5; 3, Pd^0S6. **b** Double logarithmic plots of the spectra of TDABr stabilized Pd^0 nanoparticles in THF (normalized at $\lambda = 450$ nm with $A = 1$) at different Pd^0 concentrations: 1, Pd^0S4; 2, Pd^0S5; 3, Pd^0S6

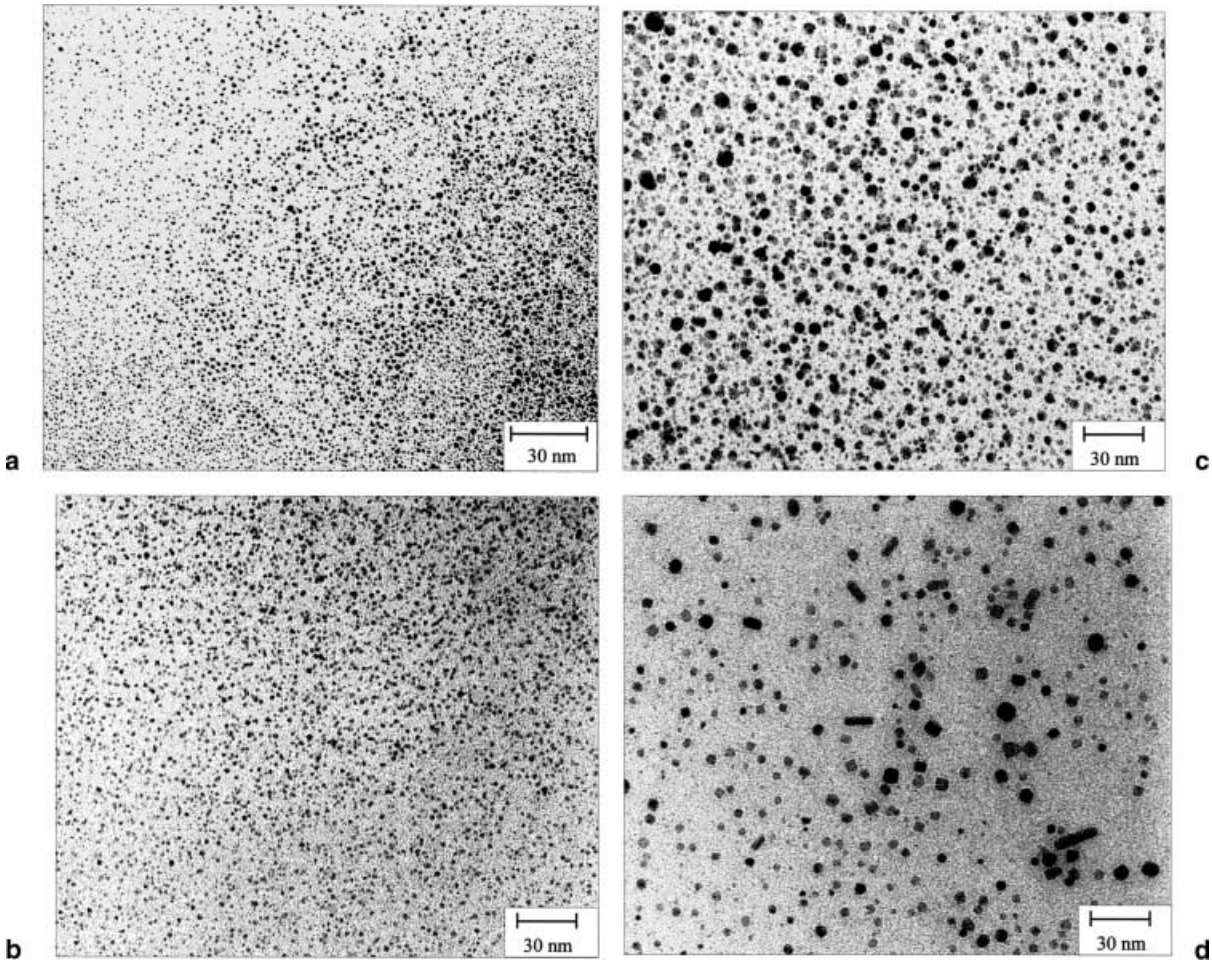

Fig. 11a–d Transmission electron micrographs of Pd^0 nanoparticles: **a** Pd^0S3; **b** Pd^0S4; **c** Pd^0S5; **d** Pd^0S6

(contraction) by association processes (appearance of clusters and aggregates).

The molar excess volumes of THF-surfactant-water microemulsions (SW) are considerably lower than those of the ethanol-containing systems (Fig. 4). In microemulsions containing water, V_m^E decreased further as the amount of water and surfactant increased. The reason for this is that, at higher surfactant concentrations, the amount of surfactant in the water/THF (liquid/liquid) interfacial layer increases, enhancing the tendency of surfactant molecules to associate.

When the radius of the microemulsion droplet is calculated from the ratio of polar liquid to surfactant by Eq. (3), the relations shown in Figs. 5 and 6 are obtained. The excess volumes increase with increasing amounts of ethanol but remain negative, indicating increasingly loosening associations. This means that, in contrast with aqueous systems, in the presence of ethanol the orientation of surfactants is suppressed. The densities of systems containing THF and surfactant increased after addition of $Pd(OAc)_2$. On addition of ethanol, the values were reduced (due to the lower density of ethanol) (Figs. 7a, b). The density of Pd^0 sols S4, 5, 6 increases with increasing Pd content (Fig. 8a). In all cases, however, the calculated excess volumes are large negative values, decreasing with increasing Pd^0 content (Fig. 8b). This means that the appearance of the solid/liquid interface due to the formation of the nanoparticles induces the orientation of the surfactant molecules in the adsorption layer on the surface of Pd^0. The adsorption of surfactants in layers stabilizing the particles results in a substantial contraction, the extent of which decreases with increasing particle size.

UV-VIS spectroscopy

According to the data published by Reetz et al. [27], in the case of Pd clusters with diameters of $d = 4.1$ nm, 2.3 nm, and 1.4 nm (determined by TEM measurements) the corresponding slopes (S) of the $\lg A$–$\lg\lambda$ curve are 3.6, 2.6 and 1.6, respectively. Absorption spectra [$A = f(\lambda)$] of Pd^0 sols were recorded in 10-mm quartz cuvettes in the range 300–600 nm

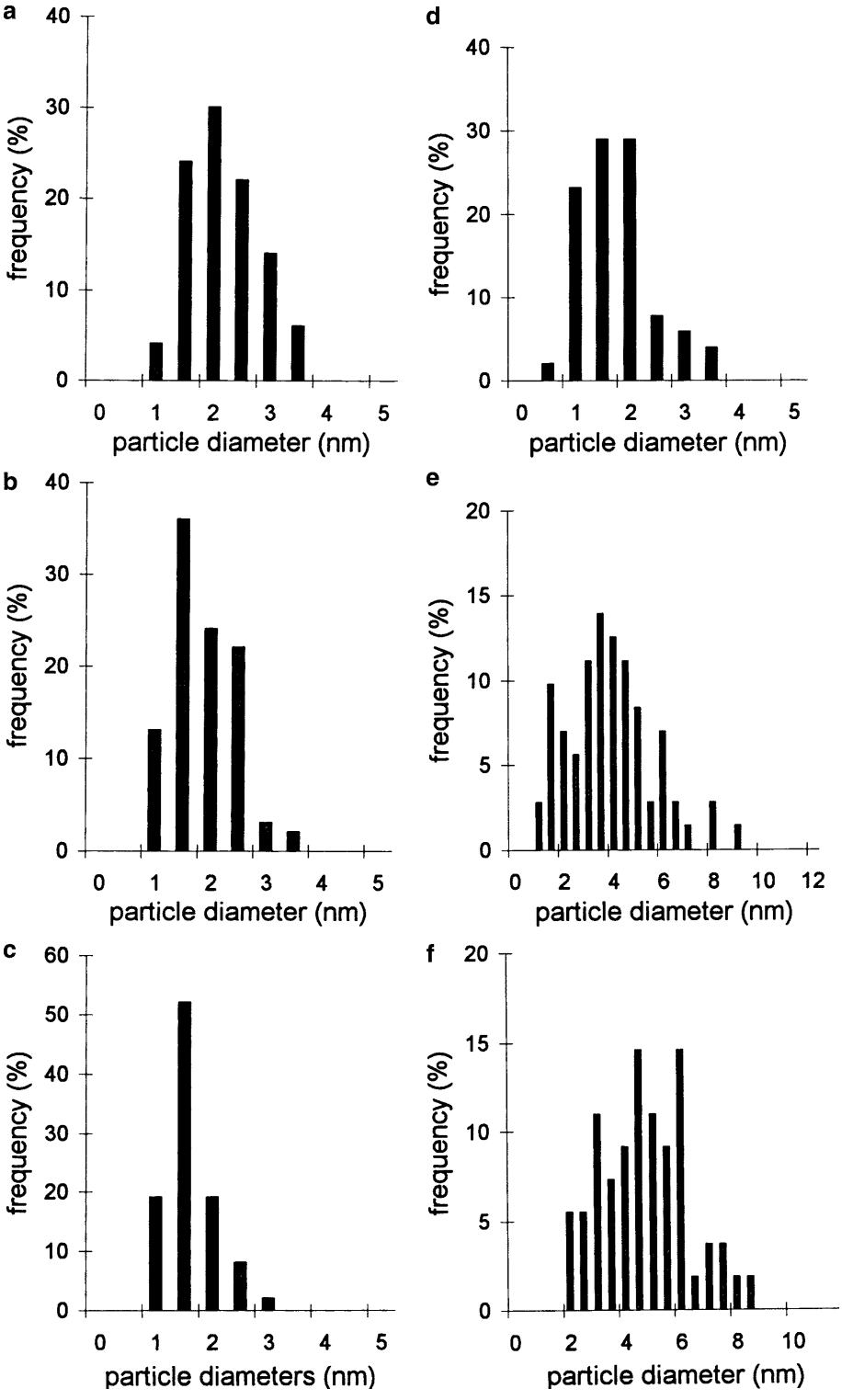

Fig. 12a–f Size histograms of Pd^0 nanoparticles: **a** Pd^0 S1; **b** Pd^0S2; **c** Pd^0S3 reduced in ethanol at various Pd^0 concentration; **d** Pd^0S4; **e** Pd^0S5; **f** Pd^0S6 prepared in THF/$TDABr/H_2O$ systems at various Pd^0 concentrations

with the THF/surfactant/ethanol as reference. For Pd^0 nanoparticles a system with $W_0 = 13.5$, $r = 12$ nm was selected in order to check whether a particle size identical with the calculated droplet size is obtained. The amount of $Pd(Ac)_2$ present in the THF/surfactant solution was varied within the concentration range of 9.1–18.2 mmol/l (Table 2) and ethanol was used as a reducing agent.

The highly concentrated sols were diluted 100-fold before spectroscopy. After normalizing absorbance values to $\lambda = 450$ nm, lgA was plotted vs lgλ and the particle sizes were calculated from the slope of the straight line (Figs. 9 and 10a, b). Exponential regression functions were next fitted to the data; the slopes and the corresponding particle sizes calculated according to the formula, $d(nm) = 0.5846 \times e^{0.5373S}$ are as follows: 1. Pd^0S1: $m = -2.378$, $d = 2.10$ nm; 2. Pd^0S2: $m = -2.123$, $d = 1.83$ nm; 3. Pd^0S3: $m = -2.097$, $d = 1.80$ nm. Increasing the amount of Pd in the ethanol droplets surrounded by surfactants reduced the particle size, since the rate of nucleation is enhanced by higher Pd^{2+} concentrations.

Aqueous microemulsions of $PdCl_2$ were measured in 10-mm quartz cuvettes. The following series of data was obtained at increasing Pd^{2+} concentrations (0.9–1.8 mmol/l): 4. Pd^0S4: $m = -3.889$, $d = 4.73$ nm; 5. Pd^0S5: $m = -5.732$, $d = 12.78$; 6. Pd^0S6: $m = -6.9267$, $d = 24.16$ nm, i.e., increasing amounts of Pd increased the particle size, since low precursor concentrations favor increased rates of nucleus growth, leading to the formation of larger nanocrystallites (see TEM pictures).

Analysis of the TEM investigations

The transmission electron micrographs are presented in Figs. 11a–d and the determination of size distribution functions are displayed in Figs. 12a–f.

We consider the TEM results of samples $Pd^0S1,2,3$ as proof for the formation of several Pd^0 nanoparticles inside one droplet, resulting in the rearrangement of the protective surfactant layer to cover the metal clusters emerging in the course of reduction.

By the evidence of these TEM pictures, the average particle sizes in $Pd^0S1,2,3$ sols in THF medium are $d_{ave}(Pd^0S1) = 1.84$ nm; $d_{ave}(Pd^0S2) = 1.51$ nm; $d_{ave}(Pd^0S3) = 1.30$ nm. The average particle size decreases with increasing palladium content, which is presumably due to the enhanced rate of nucleation in the course of ethanol reduction. Consequently, the rate of nucleation exceeds that of nucleus growth. The THF/surfactant systems are highly stable: they may be stored for several months without aggregation or any change in particle size. In inverse microemulsions containing water droplets (samples $Pd^0S4,5,6$), particle sizes calculated from TEM pictures are $d_{ave}(Pd^0S4) = 2.02$ nm; $d_{ave}(Pd^0S5) = 4.10$ nm; $d_{ave}(Pd^0S6) = 4.92$ nm. Particle size increases with increasing Pd^0 content and the system becomes increasingly polydisperse. There is a close correlation for ethanolic system in the particle diameters between TEM and spectroscopic method, but we do not find a correlation for aquatic systems because of the aggregation of nanoparticles.

Conclusions

Structural changes in microemulsions due to changes in composition were quantified by density measurements (determining the excess volumes). All excess volumes obtained were negative, which means that the introduction of surfactants brings about association on the liquid/liquid interface. Association results in a marked increase in the excess volume in aqueous systems, while in ethanol a certain "loosening" of the aggregated structure is observed. The magnitude of excess volumes was a function of droplet size and the surfactant concentration. The formation of Pd nanoparticles resulted in negative excess volumes since the surfactants are adsorbed on the surface of the particles. Particles prepared in systems the compositions of which, according to model calculations, ensured the formation of 10-nm adducts, proved to be considerably smaller than expected. In sols formed in THF/surfactant/ethanol microemulsions, the particle size decreased with increasing Pd^0 content, due to the more favorable ratio of nucleation rate vs nucleus growth rate resulting and higher rates of nucleation. In sols formed in THF/surfactant/water microemulsions, the particle size increased with increasing Pd^0 content. At lower precursor concentrations particle growth is favored and the effect of surfactants is less marked in water droplets in ethanol.

References

1. Dékány I, Turi L, Tombácz E, Fendler JH (1995) Langmuir 11:2285
2. Dékány I, Nagy L, Turi L, Király Z, Kotov NA, Fendler JH (1996) Langmuir 12(15):3709
3. Dékány I, Túri L, Szucs A, Király Z (1998) Colloids Surf A 141(3):405
4. Pillai V, Kumar P, Hou MJ, Ayyub, Shah DO (1995) Adv Colloid Interface Sci 55:241
5. Schulman HH, Staeckenius W, Prince LM (1959) J Phys Chem 63:7716
6. Lianos P, Thomas JK (1986) Chem Phys Lett 125:299
7. Nagy JB (1989) Colloids Surf 35:201
8. Pillai V, Kumar P, Multani MS, Shah DO (1993) Colloids Surf A 80:69
9. Kumar P, Pillai V, Shah DO (1992) J Magn Mag Mater 116:L229
10. Kumar P, Pillai V, Shah DO (1993) J Mat Sci Lett 12:162
11. Kurihara K, Hizling J, Stenius P, Fendler JH (1983) J Am Chem Soc 105:2574
12. Kotlachyck M, Chen SH, Huang JS, Kim MW (1984) Phys Rev A 29: 2054
13. Ben Azouz I, Ober R, Nakache E, Williams CE (1992) Colloids Surf 69:87
14. Faure A, Tistchenko AM, Zemb T, Chachaty C (1985) J Phys Chem 3373
15. Fennel Evans D, Wennerström H (1994) The colloidal domain. VCH Publishers, Weinheim, New York, Chap. 11, p 461

16. Herrmann CU, Würz U, Kahlweit M (1978) Ber Bunsenges Phys Chem 82:56
17. Karayigitogh CF, Tata M, John VT, McPherson GL (1994) Colloid Surf A Engl Aspects 82:151
18. Bönnemann H, Brijoux W, Brinkmann R, Fretzen R, Joussen T, Köppler R, Korall B, Neitler P, Richter J (1994) J Mol Catal 86:129
19. Bönnemann H, Brijoux W, Joussen T (1990) Angew Chem Int Ed Engl 29:256
20. Bönnemann H (1994) Stud Surf Sci Catal 91:185
21. Bönnemann H, Brijoux W, Brinkmann R, Dinjous E, Joußen T, Korall B (1991) Angew Chem Int Ed Engl 30:1312
22. Bönnemann H, Bogdanovic B, Brinkmann R, He DW, Spliethoff B (1983) Angew Chem Ed Engl 22:728
23. Esumi K, Shiratori M, Ishizuka H, Tano T, Torigoe K, Meguro K (1991) Langmuir 7:457
24. Fink J, Kiely CJ, Bethell D, Schiffrin DJ (1998) Chem Mater 10:922
25. Meguro K, Torizuka M, Esumi K (1988) Chem Soc Jpn 61:341
26. Boutonnet M, Kizling J, Stenius P (1982) Colloids Surf 5:209
27. Reetz MT, Helbig W, Quasier SA (1996) In: Fürstner A (ed) Active metals preparation, characterization, applications. VCH, Weinheim, New York